

A HIGH-ORDER HYBRIDIZABLE DISCONTINUOUS GALERKIN METHOD FOR GAS KINETIC EQUATION

WEI SU¹, PENG WANG¹, YONGHAO ZHANG¹ AND LEI WU¹

¹ James Weir Fluids Laboratory, Department of Mechanical and Aerospace Engineering
University of Strathclyde, G1 1XJ Glasgow, United Kingdom
lei.wu.100@strath.ac.uk

Key words: Hybridizable Discontinuous Galerkin, Boltzmann Equation, Kinetic Model, Rarefied Gas Flow

Abstract. The high-order hybridizable discontinuous Galerkin method is used to find the steady-state solution of the linearized Shakhov kinetic model equations on two-dimensional triangular meshes. The perturbed velocity distribution function and its traces are approximated in the piece-wise polynomial space on the triangular meshes and the mesh skeletons, respectively. By employing a numerical flux that is derived from the first-order upwind scheme and imposing its continuity on the mesh skeletons, global systems for unknown traces are obtained with a few coupled degrees of freedom. The steady-state solution is reached through an implicit iterative scheme. Verification is carried out for a two-dimensional thermal conduction problem. Results show that the higher-order solver is more efficient than the lower-order one. The proposed scheme is ready to extended to simulate the full Boltzmann collision operator.

1 INTRODUCTION

In a wide range of applications, the non-equilibrium rarefied gas flows are required to be predicted through accurate physical models and efficient numerical methods. The degree of rarefaction is characterized by the Knudsen number (Kn), the ratio of the mean free path λ to the flow characteristic dimension H [1]. For Knudsen numbers much smaller than one, the Navier-Stokes (NS) equations are valid. However, when $Kn > 0.001$, the non-slip boundary condition breaks down. Furthermore, for larger Knudsen numbers, the shear stress and heat flux in the hydrodynamic models cannot be simply expressed in terms of the lower-order macroscopic quantities. Thus models based on the kinetic theory are required. In kinetic theory, the velocity distribution function (VDF) of molecules in dilute gas is mathematically described by the Boltzmann equation, which is valid for the entire range of Knudsen number. Two categories of numerical approaches have been developed for the simulation of the Boltzmann equation. One is the direct simulation Monte Carlo method [1] that uses a collection of particles to mimic the molecular behavior stochastically, and the other is the deterministic method, which relies on the discretization of the governing equations over computational grids [2]. Generally

speaking, the particle-based methods are efficient and robust for high-speed flows, while the deterministic methods are promising for low-speed flows.

In the past decades, due to the rapid development of micro-electro-mechanical systems and the shale gas revolution in North America, extensive works have been devoted to constructing efficient deterministic schemes. These methods often adopt a numerical quadrature to approximate the integration with respect to molecular velocity on a discrete set of velocities. Then, the VDF, which is discrete in the velocity space but continuous in the spatial space and time, is resolved by the finite difference method (FDM), finite volume method (FVM), and finite element method (FEM) [3, 4, 5]. Compared to the (NS) equations, numerical simulation of the Boltzmann equation is expensive in terms of computation time and memory consumption. This is mainly due to the fact that additional dimensions in the molecular velocity space are discretized, resulting in a system of governing equations for each discrete VDF.

Great efforts have been devoted to reducing the computational consumption in various aspects, including the development of high-order discretization or automatically adaptive refinement in the spatial and velocity spaces [6, 7, 8]. In recent years, the high-order discontinuous Galerkin (DG) finite element methods have been applied to the gas kinetic model equations [9], and the linearized/full Boltzmann equations [10, 11, 12] for the simulation of non-equilibrium gas flows. For the simulation of a rarefied Couette flow, it has been shown that the second-order Runge-Kutta DG (RKDG) method is faster than a second-order FVM scheme by one order of magnitude [9]. However, the third-order RKDG solver is not more efficient than the lower-order one. This is probably due to two facts. Firstly, the higher-order scheme needs to resolve larger number of degrees of freedom. Secondly, since it is an explicit time marching scheme, higher-order solver needs large number of iterative steps to find the steady solution.

A new DG method, called hybridizable discontinuous Galerkin (HDG) method is then proposed to overcome the disadvantage [13]. By producing a final system in terms of the degrees of freedom in approximating traces of the field variables, HDG could significantly reduce the number of global coupled unknowns, since the trace is defined on the cell interfaces and has single-value. This advantage is prominent for steady and implicit solver, especially for gas kinetic simulation, where a cumbersome system of control equations needed to be solved. To date, the majority of HDG applications in fluid dynamics includes convection-diffusion flow [13], stokes flow [14], wave propagation problem [15] and incompressible/compressible NS flows [16, 17, 18]. In this paper, for the first time, the HDG method is designed for the gas kinetic equation. The remainder of the paper is organized as follows. In Section 2 the gas kinetic equation, as well as the numerical method are described including the discrete velocity model, HDG formulation, implementation of boundary condition and implicit iterative scheme. Two different verification problems are presented in Section 3 together with the analysis of computational performance. Conclusions are summarized in Section 4.

2 NUMERICAL METHOD

2.1 Gas Kinetic equation

The Boltzmann equation describes the evolution of VDF in dependence of spatial position, molecular velocity and time. In Cartesian coordinates, it has the form of:

$$\frac{\partial f}{\partial t} + \mathbf{v} \cdot \frac{\partial f}{\partial \mathbf{x}} + \mathbf{a} \cdot \frac{\partial f}{\partial \mathbf{v}} = \mathcal{C}. \quad (1)$$

Here, $\mathbf{v} = (v_1, v_2, v_3)$ is the molecular velocity normalized by the most probable speed $v_m = \sqrt{2RT_0}$ at the reference temperature T_0 , where R is the gas constant; $\mathbf{x} = (x_1, x_2, x_3)$ is the spatial coordinate normalized by the characteristic flow length H ; $\mathbf{a} = (a_1, a_2, a_3)$ is the external acceleration normalized by v_m^2/H ; t is the time normalized by H/v_m ; $f(t, \mathbf{x}, \mathbf{v})$ is the VDF normalized by n_0/v_m^3 , where n_0 is the average number density of gas molecules at the reference temperature; finally, \mathcal{C} is the collision operator, which describes the change in VDF resulting from binary collisions.

Due to complexity of the collision operator, the full Boltzmann equation is amenable to analytical solutions only for few special cases. In practice, deterministic solution is commonly sought for gas kinetic models that reduce $\mathcal{C}(f)$ to simpler collision operators: frequently used are the Bhatnagar-Cross-Krook (BGK) [19], ellipsoidal statistical BGK [20], and Shakhov models [21]. Here, we describe the numerical scheme based on the linearized kinetic model equation. When the flow velocity is sufficiently small compared to v_m , and the external acceleration is also small, we can linearized the VDF about the global equilibrium state f_{eq} as:

$$f = f_{\text{eq}}(1 + h), \quad f_{\text{eq}} = \frac{\exp(-|\mathbf{v}|^2)}{\pi^{3/2}}, \quad (2)$$

and the perturbed VDF $h(\mathbf{x}, \mathbf{v})$ is governed by the following linearized Shakhov kinetic model equation[22]:

$$\mathbf{v} \cdot \frac{\partial h}{\partial \mathbf{x}} - 2\mathbf{a} \cdot \mathbf{v} = \frac{\sqrt{\pi}}{2Kn} (\mathcal{L} - h), \quad (3)$$

where the perturbed local equilibrium state is given by:

$$\mathcal{L}(\mathbf{v}) = \varrho + 2\mathbf{u} \cdot \mathbf{v} + \tau \left(|\mathbf{v}|^2 - \frac{3}{2} \right) + \frac{4(1 - Pr)}{5} \mathbf{v} \cdot \mathbf{q} \left(|\mathbf{v}|^2 - \frac{5}{2} \right), \quad (4)$$

where, ϱ is the perturbed number density, $\mathbf{u} = (u_1, u_2, u_3)$ is the macroscopic flow velocity normalized by v_m , τ is the perturbed gas temperature, $\mathbf{q} = (q_1, q_2, q_3)$ is the heat flux normalized by $p_0 v_m$ with p_0 being the pressure at the reference temperature, and Pr is the Prandtl number.

Note that we have omitted the derivative with respect to the time in Eq. (3), since we are only interested in the steady- state solution. These macroscopic gas variables are evaluated from the velocity moments of the perturbed VDF:

$$\begin{aligned}
 \varrho &= \int h f_{\text{eq}} d\mathbf{v}, \\
 \mathbf{u} &= \int \mathbf{v} h f_{\text{eq}} d\mathbf{v}, \\
 \tau &= \frac{2}{3} \int |\mathbf{v}|^2 h f_{\text{eq}} d\mathbf{v} - \varrho, \\
 \mathbf{q} &= \int \mathbf{v} \left(|\mathbf{v}|^2 - \frac{5}{2} \right) h f_{\text{eq}} d\mathbf{v},
 \end{aligned} \tag{5}$$

2.2 Discrete velocity model

The deterministic approach relies on the discrete velocity method (DVM) [23], in which a set of M_v discrete velocities $\mathbf{v}^j = (v_1^{j1}, v_2^{j2}, v_3^{j3})$ are chosen to represent the VDF. If we denote $h^j = h(\mathbf{x}, \mathbf{v}^j)$, $\mathcal{L}^j = \mathcal{L}(\mathbf{v}^j)$, and $f_{\text{eq}}^j = f_{\text{eq}}(\mathbf{v}^j)$, the linearized model equation is replaced by a system of differential equations for h^j that are discrete in the velocity space but still continuous in the spatial space:

$$\mathbf{v}^j \cdot \frac{\partial h^j}{\partial \mathbf{x}} - 2\mathbf{a} \cdot \mathbf{v}^j = \frac{\sqrt{\pi}}{2Kn} (\mathcal{L}^j - h^j), \quad j = 1, \dots, M_v. \tag{6}$$

The macroscopic variables are evaluated using some numerical quadratures.

2.3 Formulation of HDG method

In this work, we apply the HDG method to discretize the system of partial differential equations (6) in the spatial space on a two-dimensional domain $\Omega \in \mathbb{R}^2$ with boundary $\partial\Omega$ in the $x_1 - x_2$ plane. First of all, Ω is partitioned in M_{el} disjoint regular triangles: $\Omega = \cup_i^{M_{\text{el}}} \Omega_i$. Thus, the boundaries $\partial\Omega_i$ of the triangles define a group of M_{fc} faces Γ : $\Gamma = \cup_i^{M_{\text{el}}} \{\partial\Omega_i\} = \cup_c^{M_{\text{fc}}} \{\Gamma_c\}$

The HDG method provides an approximate solution to h^j on Ω_i as well as an approximation to its trace \hat{h}^j on Γ_c in some piecewise finite element spaces $\mathcal{V} \times \mathcal{W}$ of the following forms:

$$\begin{aligned}
 \mathcal{V} &= \{\varphi : \varphi|_{\Omega_i} \in \mathcal{P}^k(\Omega_i), \forall \Omega_i \subset \Omega\}, \\
 \mathcal{W} &= \{\psi : \psi|_{\Gamma_c} \in \mathcal{P}^k(\Gamma_c), \forall \Gamma_c \subset \Gamma\},
 \end{aligned} \tag{7}$$

where $\mathcal{P}^k(D)$ denotes the space of k -th order polynomials on a domain D . Before describing the HDG formulation, we first define a collection of index mapping functions [24] that allow us to relate the local edge of a triangle, namely $\partial\Omega_i^e$ to a global face Γ_c . Since the e -th edge of the triangle $\partial\Omega_i$ is the c -th face Γ_c , we set $\sigma(i, e) = c$ so that $\partial\Omega_i^e = \Gamma_{\sigma(i, e)}$. Similarly, since the interior face $\Gamma_c \in \Gamma \setminus \partial\Omega$ is the intersection of the two triangles, namely left triangle Ω_{i^-} and right triangle Ω_{i^+} , we set $\eta(c, +) = i^+$ and $\eta(c, -) = i^-$, then we can denote $\Gamma_c = \partial\Omega_{\eta(c, +)} \cap \partial\Omega_{\eta(c, -)}$. At a boundary face $\Gamma_c \in \partial\Omega$, we say that only the right triangle is involving.

The HDG method solves problem in two steps [13]. First, a global problem is setup to determine the trace \hat{h}^j on Γ . Then, a local problem with \hat{h}^j as boundary condition on $\partial\Omega_i$ is solved element by element to obtain the solutions of h^j . Generally speaking, when moving from the interior of the triangle element Ω_i to its boundary $\partial\Omega_i$, \hat{h}^j defines what the value of h^j on the boundary should be. In the HDG method, it is assumed that \hat{h}^j is singled-valued on each face.

Introducing (\cdot) and $\langle \cdot \rangle$ as $(a, b)_D = \int_{D \subset \mathbb{R}^2} (a \cdot b) dx_1 dx_2$ and $\langle a, b \rangle_D = \int_{D \subset \mathbb{R}^1} (a \cdot b) d\Gamma$, respectively, the weak formulation of Eq. (6) for the VDF h^j in each element Ω_i is:

$$-(\nabla\varphi, \mathbf{v}^j h^j)_{\Omega_i} + \sum_{e=1}^3 \langle \varphi, \hat{\mathbf{F}} \cdot \mathbf{n} \rangle_{\partial\Omega_i^e} + (\varphi, \delta h^j)_{\Omega_i} = (\varphi, s^j)_{\Omega_i}, \quad \text{for all } \varphi \in \mathcal{V}, \quad (8)$$

where $\hat{\mathbf{F}}$ is the numerical trace of the flux, \mathbf{n} is the outward unit normal vector, and $s^j = \mathcal{L}^j - X_P v_3^j$. In practice, the numerical trace of the flux is defined as [25]:

$$\hat{\mathbf{F}}^j \cdot \mathbf{n} = \mathbf{v}^j \cdot \mathbf{n} \hat{h}^j + \alpha (h^j - \hat{h}^j), \quad (9)$$

where α is a stabilization parameter [16] on each edge $\partial\Omega_i^e$. Here, we evaluate α as: $\alpha = |\mathbf{v}^j \cdot \mathbf{n}|$.

By inserting Eq. (9) into Eq. (8), we find the solution of h^j on each triangle as a function of the \hat{h}^j . In matrix form, it is written as

$$\mathbf{H}^{i,j} = [\mathbf{A}^{i,j}]^{-1} \mathbf{S}^{i,j} + [\mathbf{A}^{i,j}]^{-1} \hat{\mathbf{A}}^{i,j} \hat{\mathbf{H}}^{i,j}, \quad (10)$$

where $\mathbf{H}^{i,j}$ ($\hat{\mathbf{H}}^{i,j}$) are the vectors of degrees of freedom of h^j (\hat{h}^j) on Ω_i ($\partial\Omega_i$). The coefficient matrices $\mathbf{A}^{i,j}$, $\mathbf{S}^{i,j}$ and $\hat{\mathbf{A}}^{i,j}$ are given in the Appendix in detail.

The global problem, used for the determination of \hat{h}^j , is obtained by imposing the continuity of the normal fluxes at cell interfaces. For all $\psi \in \mathcal{W}$, the weak formulation is:

$$\begin{aligned} \langle \psi, \hat{\mathbf{F}} \cdot \mathbf{n}_{\eta(c,+)} \rangle_{\Gamma_c} + \langle \psi, \hat{\mathbf{F}} \cdot \mathbf{n}_{\eta(c,-)} \rangle_{\Gamma_c} &= 0, \quad \text{on } \Gamma \setminus \partial\Omega, \\ \langle \psi, \hat{\mathbf{F}} \cdot \mathbf{n}_{\eta(c,+)} \rangle_{\Gamma_c} + \langle \psi, \hat{\mathbf{G}} \cdot \mathbf{n} \rangle_{\Gamma_c} &= 0, \quad \text{on } \Gamma \cap \partial\Omega, \end{aligned} \quad (11)$$

where $\hat{\mathbf{F}} \cdot \mathbf{n}_{\eta(c,\pm)}$ denote the numerical fluxes calculated from the left and right triangles, and $\hat{\mathbf{G}} \cdot \mathbf{n}$ is the flux defined over the boundary $\partial\Omega$ flowing into the computational domain. Note that the implementation of the boundary condition is equivalent to the standard Neumann boundary condition. By inserting the definition of the numerical flux, i.e. Eq. (9), we obtain the matrix system for the global problem:

$$\begin{aligned} \hat{\mathbf{B}}^{c,j} \hat{\mathbf{H}}^{c,j} &= \mathbf{B}^{\eta(c,+),j} \mathbf{H}^{\eta(c,+),j} + \mathbf{B}^{\eta(c,-),j} \mathbf{H}^{\eta(c,-),j}, \quad \text{on } \Gamma \setminus \partial\Omega, \\ \hat{\mathbf{B}}^{c,j} \hat{\mathbf{H}}^{c,j} &= \mathbf{B}^{\eta(c,+),j} \mathbf{H}^{\eta(c,+),j} + \hat{\mathbf{S}}^{c,j}, \quad \text{on } \Gamma \cap \partial\Omega, \end{aligned} \quad (12)$$

where $\hat{\mathbf{H}}^{c,j}$ is the vector of degrees of freedom of \hat{h}^j on Γ_c . Other coefficient matrices are given in Appendix in detail.

After eliminating the unknowns $\mathbf{H}^{i,j}$ with Eq. (10) and assembling the Eq. (13) over all the faces, the global problem becomes: $\mathbb{K}^j \hat{\mathbf{H}}^j = \mathbb{R}^j$, where $\hat{\mathbf{H}}^j$ is the vector of degrees of

freedom of \hat{h}^j on all the faces Γ , \mathbb{K}^j is the global matrix of the linear system of equations, and \mathbb{R}^j is the vector in the right-hand side of the system. It is noted that the linear system of equations is highly sparse, in which only face unknowns that involve in two adjacent triangles are coupled at each row. The system could be solved by robust direct solver for sparse unsymmetrical linear systems, e.g. the package PARDISO [26]. Once the values of \hat{h}^j are obtained, an element-by-element reconstruction of the approximation of h^j is implemented according to Eq. (10).

Before describing the implementation of boundary condition, we take an insight into the form of the numerical fluxes. If inserting the expression of flux (9) into the continuity equation (12) at interior faces, we immediately obtained:

$$\langle \psi, \hat{h}^j \rangle = \frac{1}{2} \langle \psi, h_{\eta(c,+)}^j + h_{\eta(c,-)}^j \rangle. \quad (13)$$

That is, the trace \hat{h}^j at interior face is equal, in a weak sense, to the average of $h_{\eta(c,\pm)}^j$, which are evaluated at the interface from the left and right triangles, respectively. Then we obtain an equivalent expression for $\hat{\mathbf{F}} \cdot \mathbf{n}$:

$$\hat{\mathbf{F}} \cdot \mathbf{n}_{\eta(c,\pm)} = \begin{cases} \mathbf{v}^j \cdot \mathbf{n}_{\eta(c,\pm)} h_{\eta(c,\pm)}^j, & \mathbf{v}^j \cdot \mathbf{n}_{\eta(c,\pm)} \geq 0 \\ \mathbf{v}^j \cdot \mathbf{n}_{\eta(c,\mp)} h_{\eta(c,\mp)}^j, & \mathbf{v}^j \cdot \mathbf{n}_{\eta(c,\pm)} < 0 \end{cases}, \quad (14)$$

which is exactly the upwind scheme.

2.4 Implementation of boundary condition

In order to complete the formulation, we need to specify the flux $\hat{\mathbf{G}} \cdot \mathbf{n}$ at boundary $\partial\Omega$. To be consistent with the evaluation the fluxes at interior faces, we calculate the boundary flux as:

$$\hat{\mathbf{G}} \cdot \mathbf{n} = \mathbf{v}^j \cdot \mathbf{n} \hat{h}^j + \alpha \left(g^j - \hat{h}^j \right), \quad (15)$$

where g^j is the boundary value of h^j and \mathbf{n} is the outward unit normal vector at the boundary pointing into the flow field. In this paper, the fully diffuse boundary condition is used to determine the perturbed VDF g^j at the solid surface. Suppose the solid wall is static and has the temperature T_0 , the perturbed VDF for the reflected molecules at the wall (i.e., when $\mathbf{v}^j \cdot \mathbf{n} > 0$) is given by $g^j = -\frac{1}{2}\tau_w - 2\sqrt{\pi} \sum_{\mathbf{v}^j \cdot \mathbf{n} < 0} (\mathbf{v}^j \cdot \mathbf{n}) f_{\text{eq}}^j h^j \Delta \mathbf{v}^j + \tau_w \left(|\mathbf{v}^j|^2 - \frac{3}{2} \right)$. Other type of boundary conditions, such as the Maxwell diffuse-specular boundary condition with given tangential momentum accommodation coefficient, symmetry boundary, periodic boundaries, as well as far-pressure inlet/outlet boundary could be incorporated straightforwardly [9, 30].

2.5 Implicit iterative scheme

Note that the linearized perturbed equilibrium distribution \mathcal{L}^j depends on the macroscopic variables that are evaluated from the unknown perturbed VDF h^j . The system of Eqs. (6) are commonly solved by the following implicit iterative scheme:

$$\frac{\sqrt{\pi}}{2Kn} h^{j,(t+1)} + \mathbf{v}^j \cdot \frac{\partial h^{j,(t+1)}}{\partial \mathbf{x}} = \frac{\sqrt{\pi}}{2Kn} \mathcal{L}^{j,(t)} + 2\mathbf{a} \cdot \mathbf{v}^j, \quad j = 1, \dots, M_v. \quad (16)$$

where the superscripts (t) and $(t + 1)$ represent two consecutive iteration steps. The iteration is terminated when the convergence to the steady solution is achieved. The convergence criterion is that the global relative residual in a flow macroscopic property Q between two successive iterative steps is less than a threshold value ϵ .

3 RESULTS AND DISCUSSIONS

For verification, we consider a two-dimensional heat conduction problem. As shown in Figure 1, the gas flow is contained in a square cavity, whose three boundaries are maintained at $\tau_1 = 0$ and the fourth side is at $\tau_2 = 0.02$. The flow is initiated within the slip flow regime with $Kn = 0.01$. The computational domain is set as $\Omega = [0, 0.5] \times [0, 1]$ due to symmetry. The bottom, top and left boundaries are fully diffuse walls, while the boundary at $x_1 = 0.5$ is symmetric boundary. The HDG method of k up to 3 is employed to solve the linearized Shakhov model equation. The perturbed temperature τ is used to evaluate the iterative residual, and the threshold value is set as $\epsilon = 10^{-10}$. For the discretization of velocity space, the Gauss-Legendre quadrature is employed, and 8 points are assigned in each direction, and further refinement of the velocity grid would only improve the solutions by a magnitude no more than 0.5%. The entire tests are done in double precision on a workstation with Intel Xeon-E5-2680 processors and 132 GB RAM. The system of the control equations for each discrete h^j are solved on 4 CPUs through OpenMP parallel interface. During iteration, we call the relative routines in Intel[®] Math Kernel Library (MKL) to invert the matrix. Moreover, to solve the HDG global equations, we call the direct sparse solver, Intel[®] MKL PARDISO. In the slip flow regime, the distribution of gas temperature could also be described by the Laplace equation combined with a temperature jump condition [31]:

$$\frac{\partial^2 \tau}{\partial x_1^2} + \frac{\partial^2 \tau}{\partial x_2^2} = 0, \quad (17)$$

$$\tau - \tau_w = 0.982 \frac{2\gamma}{\gamma + 1} \frac{\gamma}{Pr} \left(\frac{\partial \tau}{\partial x} \right)_w, \quad \text{at } \partial\Omega \quad (18)$$

where, γ is the specific heat capacity ratio, and $(\frac{\partial \tau}{\partial x})_w$ is the temperature gradient in the perpendicular direction at the wall. For verification, the temperature distribution from the HDG solver are compared with the one from the Laplace equation, which is solved by the FEM solver in MATLAB[®] PDE tool box with linear approximation polynomial. Total 4145 triangle elements with refinement near the upper corners are used on the full domain to obtain accurate result.

Figure 2 shows the perturbed temperature contours obtained by the HDG solver with different approximation polynomials on spatial grids with increasing triangles. The results are compared with the one obtained from the Laplace equation. It is vividly demonstrated the convergence history of the solution on successively refined mesh.

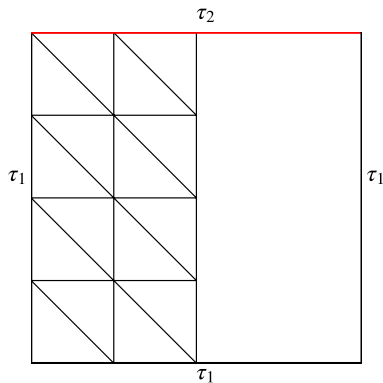


Figure 1: Schematics of the geometry and mesh for the two-dimensional conduction problem.

Table 1: Two-dimensional conduction problem: demonstration of the performance of the HDG solver in terms of the average relative L_1 error (compared with the solutions of the Laplace equation), the number of iterations (Itr denotes the number of iteration steps to reach the convergence criterion $R < 10^{-10}$), and the computational time t_c .

k	M_{el}	L_1 error	Itr	t_c , [s]
1	16	1.01×10^{-1}	4509	226.1
	36	4.41×10^{-2}	4655	335.0
	64	2.58×10^{-2}	4702	558.3
	100	1.90×10^{-2}	4721	861.6
2	4	8.78×10^{-2}	4654	204.8
	16	2.27×10^{-2}	4741	373.4
	36	1.77×10^{-2}	4745	722.8
	64	1.72×10^{-2}	4745	1399.6
3	4	3.22×10^{-2}	4743	270.8
	16	1.80×10^{-2}	4745	389.6
	36	1.78×10^{-2}	4746	1193.4
	64	1.81×10^{-2}	4746	1502.2

For the HDG, the average L_1 errors, the numbers of iterative steps, and the computational time are listed in Table 2, for various numbers of triangles and degrees of approximation polynomial. The L_1 error is estimated as: $M_p = 101 \times 201$ equidistant nodes are first distributed in the domain $[0, 0.5] \times [0, 1]$; then, the temperature at each points τ_p could be calculated from the approximating polynomials in the relevant triangles; finally, the L_1 error is $\frac{1}{M_p} \sum_p |\tau_p^{HDG} - \tau_p^L| / |\tau_p^L|$ with τ_p^L being the solution from the Laplace equation. It is found that the HDG solvers obtained the converged solution with L_1 errors is around 1.8×10^{-2} . The solvers with $k = 1, 2$ and 3 reach the results at such error level on $M_{\text{el}} = 100, 36$ and 16 triangles, respectively. In this two-dimensional problem, the number of iterative steps to find the converged result approaches to a fix values about 4745 for all solvers. The computational time to obtained solutions with 1.8% error for $k = 3$ is about 54% and 45% of that for $k = 2$ and $k = 1$, respectively.

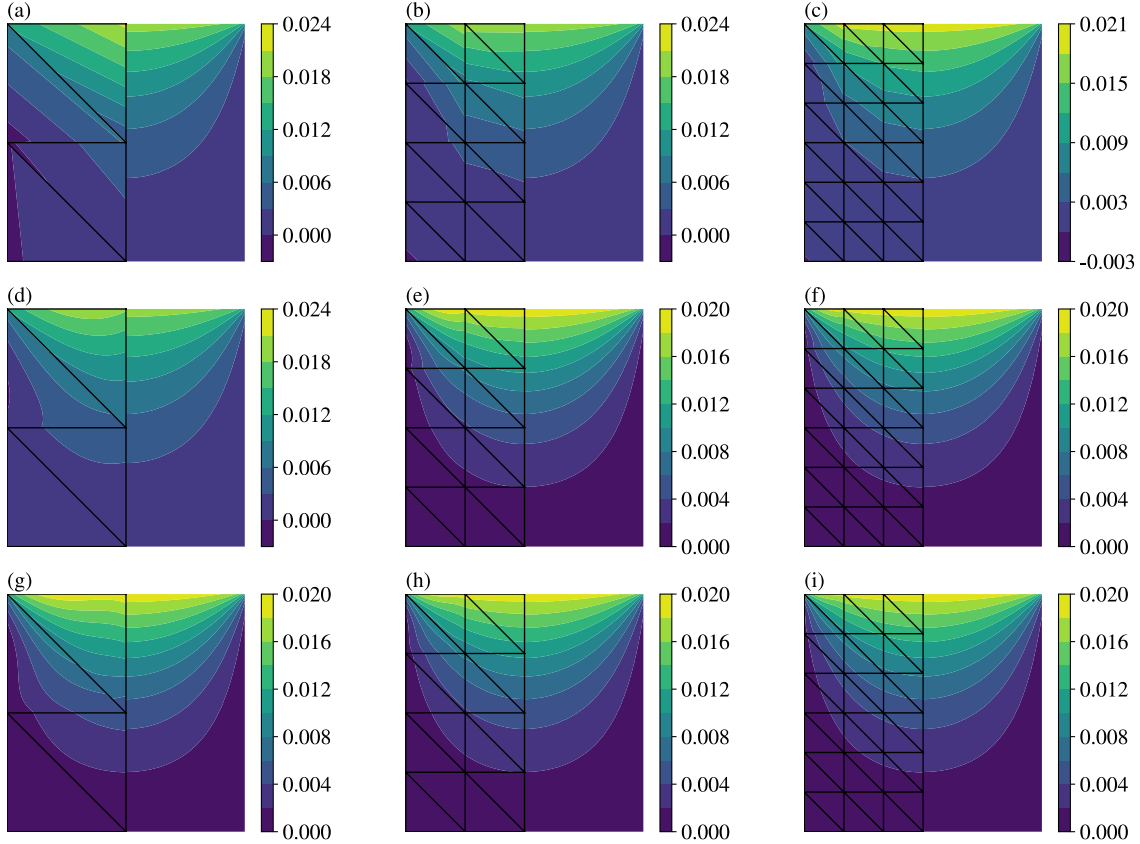


Figure 2: Perturbed temperature contours of the conduction problem. From the top to the bottom row: solutions of HDG with $k = 1 \sim 3$, respectively. On each map, left domain shows the HDG result while the right domain shows the one from the Laplace equation.

4 CONCLUSIONS

In summary, we have developed a high-order hybridizable discontinuous Galerkin method for the solution of the linearized Boltzmann BGK and Shakhov kinetic model equations on arbitrary triangular mesh. With this approach, the velocity space is first discretized using a proper quadrature rule. Then, the discrete perturbed molecular VDFs and their traces are approximated on spatial mesh and the mesh skeleton, respectively. The approximation polynomial is of degree up to 4. Based on the first-order upwind scheme, a numerical flux has been designed to evaluate the convection between adjacent cells. By imposing the continuity of the normal flux, global systems are setup in terms of only the unknown traces. Once the traces are resolved, the VDFs are updated in an element-by-element fashion. The boundary condition has been implemented equivalently to the standard Neumann boundary condition. In this way, the boundary condition could be treated in a unified framework the same as the calculation of flux on interfaces. Finally, an implicit iterative scheme is employed to find the steady solution of gas flows.

Verification has been performed for a two-dimensional thermal conduction problem in the near-continuum flow regime. The results show that, to obtain the converged steady

solution, the HDG solver with higher-order approximation polynomial requires fewer triangles thus fewer degrees of freedom of the VDF traces, while the numbers of iterative steps are almost the same for solvers with different degree of polynomials. Therefore, the higher order the solver, the less the computational time.

ACKNOWLEDGMENTS

This work is jointly funded by the Royal Society of Edinburgh and National Natural Science Foundation of China under Grant No. 51711530130. It is also financially supported by the Carnegie Research Incentive Grant for the Universities in Scotland, and the Engineering and Physical Sciences Research Council (EPSRC) in the UK under grant.

Appendix

The matrices in the local and global formulations are

$$\begin{aligned}
 \mathbf{A}_{ml}^{i,j} &= \delta(N_i^m, N_i^l)_{\Omega_i} + \sum_{e=1}^3 \alpha \langle N_i^m, N_i^l \rangle_{\partial\Omega_i} - (\mathbf{v}^j \cdot \nabla N_i^m, N_i^l)_{\Omega_i}, \\
 \hat{\mathbf{A}}_{ml}^{i,j,e} &= (\alpha - \mathbf{v}^j \cdot \mathbf{n}) \langle N_i^m, \hat{N}_{\sigma(i,e)}^l \rangle_{\partial\Omega_i^e}, \\
 \mathbf{S}_m^{i,j} &= (N_i^m, s^j)_{\Omega_i}, \\
 \hat{\mathbf{B}}_{ml}^{c,j} &= \langle \hat{N}_c^m, \hat{N}_c^l \rangle_{\Gamma_c}, \\
 \mathbf{B}_{ml}^{\eta(c,\pm),j} &= \frac{1}{2} \langle \hat{N}_c^m, N_{\eta(c,\pm)}^l \rangle_{\Gamma_c}, \\
 \hat{\mathbf{S}}_m^{c,j} &= \frac{1}{2} \langle \hat{N}_c^m, g^j \rangle_{\Gamma_c}.
 \end{aligned}$$

REFERENCES

- [1] Bird, G.A. *Molecular gas dynamics and the direct simulation*. Clarendon, 2nd Edition, 1994.
- [2] Aristov, A.A. *Direct methods for solving the Boltzmann equation and study of nonequilibrium flows*. Springer, 2001.
- [3] Yang, J. and Huang, J. Rarefied flow computations using nonlinear model Boltzmann equations. *J. Comput. Phys.* (1995) **120**:323–339.
- [4] Mieussens, L. Discrete-velocity models and numerical schemes for the Boltzmann-BGK equation in plane and axisymmetric geometries. *J. Comput. Phys.* (2000) **162**:429–466.
- [5] Kolobov, V. Arslanbekov, R. Aristov, V. Frolova, A. and Zabelok, S. Unified solver for rarefied and continuum flows with adaptive mesh and algorithm refinement. *J. Comput. Phys.* (2007) **223**:589–608.
- [6] Arslanbekov, R.R. Kolobov, V.I. and Frolova, A.A. Kinetic solvers with adaptive mesh in phase space. *AIP Conf. Proc.* (2012) **1501**:294–301.

- [7] Baranger, C. Claudel, J. Hrouard, N. and Mieussens, L. Locally refined discrete velocity grids for stationary rarefied flow simulations. *J. Comput. Phys.* (2014) **257**:572–593.
- [8] Alekseenko, A. and Josyula, E. Deterministic solution of the spatially homogeneous Boltzmann equation using discontinuous Galerkin discretizations in the velocity space. *J. Comput. Phys.* (2014) **272**:170–188.
- [9] Su, W. Alexeenko, A.A. and Cai, G. A parallel Runge-Kutta discontinuous Galerkin solver for rarefied gas flows based on 2D Boltzmann kinetic equations. *Comput. Fluids*. (2015) **109**:123–136.
- [10] Gobbert, M. Webster, S. and Cale, T. A Galerkin method for the simulation of the transient 2-D/2-D and 3-D/3-D linear Boltzmann equation. *J. Sci. Comput.* (2007) **30**:237–273.
- [11] Baker, L.L. and Hadjiconstantinou, N.G. Variance-reduced Monte Carlo solutions of the Boltzmann equation for low-speed gas flows: a discontinuous Galerkin formulation. *Int. J. Numer. Method. Fluids* (2008) **58**:381–402.
- [12] Kitzler, G. and Schberl, J. A high order space-momentum discontinuous Galerkin method for the Boltzmann equation. *Comput. Math. Appl.* (2015) **70**:1539–1554.
- [13] Cockburn, B. Gopalakrishnan, J. and Lazarov, R. Unified hybridization of discontinuous Galerkin, mixed, and continuous Galerkin methods for second order elliptic problems. *SIAM J. Num. Analy.* (2009) **47**:1319–1365.
- [14] Nguyen, N. Peraire, J. and Cockburn, B. A hybridizable discontinuous Galerkin method for stokes flow. *Comput. Method. Appl. Mech. Eng.* (2010) **199**:582–597.
- [15] Giorgiani, G. Fernández Méndez, S. and Huerta, A. Hybridizable discontinuous Galerkin p-adaptivity for wave propagation problems. *Int. J. Numer. Method. Fluids* (2013) **72**:1244–1262.
- [16] Peraire, J. Nguyen, N. and Cockburn, B. A hybridizable Discontinuous Galerkin method for the compressible Euler and Navier-Stokes equations. *Proceedings of the 48th AIAA Aerospace Science Meeting.* (2010).
- [17] Nguyen, N. Peraire, J. and Cockburn, B. An implicit high-order hybridizable discontinuous Galerkin method for the incompressible Navier-Stokes equations. *J. Comput. Phys.* (2011) **230**:1147–1170.
- [18] Moghtader, M.J. *High-order hybridizable discontinuous Galerkin method for viscous compressible flows*, Ph.D Thesis, Universitat Politècnica de Catalunya, 2016.
- [19] Bhatnagar, P.L. Gross, E.P. and Krook, M. A model for collision processes in gases. I. Small amplitude processes in charged and neutral one-component systems. *Phys. Rev.* (1954) **94**:511–525.

- [20] Holway, L.H.Jr. New statistical models for kinetic theory: methods of construction. *Phys. Fluids* (1966) **9**:1658–1673.
- [21] Shakhov, E. Generalization of the Krook kinetic relaxation equation. *Fluid Dyn.* (1968) **3**:95–96.
- [22] Cercignani C. *The Boltzmann equations and its applications*. Springer-Verlag, 1988.
- [23] Huang, A.B. and Giddens, D.P. The discrete ordinate method for the linearized boundary value problems in kinetic theory of gases. Brundin, C.L. (Ed.), *Proceedings of the 5th International Symposium on Rarefied Gas Dynamic*, (1967) **1**:481–504.
- [24] Kirby, R.M. Sherwin, S.J. and Cockburn, B. To CG or HDG: a comparative study. *J. Sci. Comput.* (2012) **51**:183–212.
- [25] Sevilla, R. and Huerta, A. *Tutorial on hybridizable Discontinuous Galerkin (HDG) for second-order elliptic problems*. Springer International Publishing, 2016.
- [26] Schenk, O. and Gärtner, K. Solving unsymmetric sparse systems of linear equations with PARDISO. *Future Gener. Comput. Syst.* (2004) **20**:475–487.
- [27] Wu, L. and Struchtrup, H. Assessment and development of the gas kinetic boundary condition for the Boltzmann equation. *J. Fluid Mech.* (2017) **823**:511–537.
- [28] Su, W. Lindsay, S. Liu, H. and Wu, L. Comparative study of the discrete velocity and lattice Boltzmann methods for rarefied gas flows through irregular channels. *Phys. Rev. E* (2017) **96**:023309.
- [29] Wang, P. Ho, M.T. Wu, L. Guo, Z. and Zhang, Y. A comparative study of discrete velocity methods for low-speed rarefied gas flows, *Comput. Fluids* (2018) **161**:33–46.
- [30] Wu, L. Zhang, J. Liu, H. Zhang, Y. and Reese, J.M. A fast iterative scheme for the linearized Boltzmann equation. *J. Comput. Phys.* (2017) **338**:431–451.
- [31] Shen, C. *Rarefied gas dynamics: fundamentals, simulations and micro flows*. Springer-Verlag, 2005.